DR HAO ZHOU (Orcid ID : 0000-0001-8138-7275)

Article type : Original Manuscript

Effects of melatonin on fatty liver disease: the role of NR4A1/DNA-PKcs/p53 pathway, mitochondrial fission and mitophagy

Hao Zhou[1, 2*], Wenjuan Du[1*], Ye Li[1], Chen, Shi[3], Nan Hu[2], Sai Ma[2], Weihu Wang[3], Jun Ren[2]

[1]Chinese PLA General Hospital, Medical School of Chinese PLA, Beijing, China

[2]University of Wyoming College of Health Sciences, Laramie, WY 82071 USA

[3]Key Laboratory of Carcinogenesis and Translational Research (Ministry of Education/Beijing),

Department of Radiation Oncology, Peking University Cancer Hospital and Institute, Beijing, China

*These authors contributed equally to this study.

This article has been accepted for publication and undergone full peer review but has not been through the copyediting, typesetting, pagination and proofreading process, which may lead to differences between this version and the Version of Record. Please cite this article as doi: 10.1111/jpi.12450

Correspondence to: Dr. Hao Zhou (e-mail: zhouhao301@outlook.com)[1], Dr. Jun Ren[2]

(e-mail: jren@uwyo.edu) and Dr. Weihu Wang[3] (e-mail: wangweihufl@outlook.com)

[1]Department of Cardiology, Chinese PLA General Hospital, Beijing, China

[2]University of Wyoming College of Health Sciences, Laramie, WY 82071 USA

[3]Department of Radiation Oncology, Peking University Cancer Hospital and Institute, Beijing, China

Abstract

Mitochondrial dysfunction has been implicated in the pathogenesis of nonalcoholic fatty liver disease (NAFLD) through poorly defined mechanisms. Melatonin supplementation has been found to protect liver function in diabetes and obesity. Here, we intensively explored the role and mechanism of melatonin in the development of NAFLD. We demonstrated that the onset of diet-induced NAFLD greatly caused NR4A1 upregulation in hepatocytes, leading to the activation of DNA-PKcs and p53. On the one hand, p53 aided Drp1 migration in the mitochondria and consequently drove mitochondrial fission. On the other hand, p53 repressed Bnip3 transcription and expression, resulting into mitophagy arrest. The excessive fission and deficient mitophagy dramatically mediated

mitochondrial dysfunction, including extensive mPTP opening, reduction in mitochondrial potential, oxidative stress, calcium overload, mitochondrial respiratory collapse and ATP shortage. However, genetic deletion of NR4A1 or DNA-PKcs could definitively reverse NAFLD progression and the mitochondrial dysfunction. Similarly, melatonin supplementation could robustly reduce the damage to liver and mitochondrial structure and function in NAFLD. Mechanistically, melatonin halted fission but recovered mitophagy via blockade of NR4A1/DNA-PKcs/p53 pathway, finally improving mitochondrial and liver function in the setting of NAFLD. Our results identify NR4A1/DNA-PKcs/p53 pathway as the novel molecular mechanism underlying the pathogenesis of NAFLD via regulation Drp1-mediated mitochondrial fission and Bnip3-related mitophagy. Meanwhile, we also confirm that melatonin has the ability to cut off the NR4A1/DNA-PKcs/p53 pathway, which confers a protective advantage to hepatocytes and mitochondria. The manipulation of NR4A1/DNA-PKcs/p53 pathway by melatonin highlights a new entry point for treating NAFLD.

KEYWORDS: Melatonin, NAFLD, NR4A1, DNA-PKcs, p53, Mitochondrial fission, Mitophagy.

1 | INTRODUCTION

Metabolic syndrome (MetS) refers to a group of metabolic alterations characterized by central obesity, dyslipidemia, elevated plasma glucose, insulin resistance, elevated blood pressure, pro-thrombotic and pro-inflammatory states[1]. Patients with MetS are also more susceptible to developing type 2 diabetes mellitus and suffer increased risks of developing cardiovascular disease. In addition, their hepatic morphology and functionality can be adversely affected leading to the development of non-alcoholic fatty liver disease (NAFLD)[2]. Hepatic morphology and functionality in NAFLD can be categorized into four different stages, including a simple steatosis, non-alcoholic steatohepatitis (NASH), fibrosis and hepatocellular carcinoma[3]. Although the exact mechanisms leading to NAFLD are not yet completely understood, mitochondrial dysfunction and energy disorders have been described as playing major roles[4]. Recently, mitochondrial fission and mitophagy have come to be considered as vital means of sustaining mitochondrial homeostasis[5]. However, little information is available to explain the role of fission and mitophagy in the progression of NAFLD.

Ample evidences have established the harmful effect of p53 on hepatic death via regulation of mitochondrial fission and mitophagy[6, 7]. p53 can shuttle from the nuclear to the cytoplasm, where it helps Drp1 translocation to the surface of mitochondria[8]. As a consequence of the interaction with

Drp1, mitochondria divide into several fragments[9]. Moreover, researchers have also profiled p53 as the transcriptional repressor of Bnip3, a receptor of mitophagy[10]. Phosphorylated p53 blunts the Bnip3 expression and renders mitophagy unresponsive to stress injury[11]. However, whether the above mechanisms are also implicated in the mitochondrial dysfunction in the development of NAFLD remains unclear.

Recent studies have found that p53 could be phosphorylated by DNA-dependent protein kinase catalytic subunit (DNA-PKcs)[12], a central enzyme involved in the repair of DNA double-strand breaks (DSB) in mammalian cells via inducing cell cycle arrest and either DNA repair or apoptosis[13]. Under physiological conditions, DNA-PKcs primarily binds to Ku80, which acts as a regulatory element to repair DSB via recognition and interaction with the broken ends of DNA[14]. Therefore, this pathway functions as an intrinsic repair signal to promote cellular survival. However, in instances of prolonged insult or irreparable cell damage, DNA-PKcs preferentially interacts with and phosphorylates p53 at Ser15 to selectively induce p53-dependent cellular apoptosis[12]. Accordingly, the DNA-PKcs/p53 pathway is an endogenous cellular clearing response. Unfortunately, excessive cell clearing would result in liver tissue injury due to functional cell loss. Whether DNA-PKcs/p53 pathway is implicated in the development of chronic metabolic liver injury is poorly understood.

Nuclear receptors represent a family of transcription factors responsible for the regulation of many intracellular pathways, such as cancer, metabolic and proliferative diseases[15]. They are termed orphan because their endogenous ligands have not yet been identified. The orphan nuclear receptor subfamily 4 group A member 1 (NR4A1) has been found to be progressively increased during the development of diabetes[16]. Higher NR4A1 levels stimulate glucose production and raise blood glucose levels[17]. Conversely, expression of an inhibitory mutant NR4A1 antagonizes gluconeogenic gene expression and lowers blood glucose levels in db/db mice. More importantly, higher NR4A1 expression blocks the interaction between DNA-PKcs and Ku80 but promotes the DNA-PKcs integration with p53, leading to the cell death in liver cancer[12, 18]. However, whether NR4A1/DNA-PKcs/p53 pathway is activated and contributes to the liver mitochondrial dysfunction and NAFLD progression is incompletely understood.

Melatonin, the principal secretory product of the pineal gland[19], has been reported to participate in the hepatic mitochondrial homeostasis in diabetic obese rats[20, 21]. Therefore, the use of melatonin to protect mitochondrial function[22], may be an effective strategy to correct their impairment and restore liver function in NAFLD[23, 24]. In the present study, we posited and analyzed the following three hypotheses: (1) whether NR4A1 is upregulated in NAFLD and amplifies DNA-PKcs/p53 pathway;

(2) whether NR4A1/DNA-PKcs/p53 signaling aggravates mitochondrial dysfunction via mitochondrial fission and mitophagy in NAFLD; (3) whether melatonin has the ability to reverse chronic metabolic liver damage via inhibition of NR4A1/DNA-PKcs/p53 pathway.

2 | MATERIAL AND METHODS

2.1 | Experimental animals and diet

All animal procedures described herein were in accordance with the Guide for the Care and Use of Laboratory Animals published by the US National Institutes of Health (NIH Publication No. 85–23, revised 1996). All experimental protocols were approved (Approval ID: 2015053) by the Ethics Committee of the Key Laboratory of Carcinogenesis and Translational Research (Ministry of Education/Beijing), Peking University Cancer Hospital and Institute, Beijing, China. Wild-type (WT) and NR4A1 knockout (NR4A1-KO) mice with a C57BL/6 background were purchased from Jackson Laboratory (Bar Harbor, ME, USA) and were bred at the Key Laboratory of Carcinogenesis and Translational Research (Ministry of Education/Beijing). To specifically knockout DNA-PKcs in liver, DNA-PKcs$^{fl/fl}$ mice were crossed with Alb^{Cre+} mice to obtain DNA-PKcs liver specific knockout mice

(DNA-PKcs^{LKO} mice). To generate the DNA-PKcs$^{fl/fl}$ mice, a LoxP site was inserted between exons 81 and 82 of a 3.6 kb Hind III - SacI fragment of the mouse Prkdc gene in a pBluescript II SK vector to give p1227 by using a QuikChange kit from Agilent Technologies (Santa Clara, CA) and the oligo PKKpnLoxP2

(5′-CCTCCCAAGTGCTGGGATTAGGTACCATAACTTCGTATAATGTATGCTATACGA AGTTATAAGGCGTGCACTACCACTGC-3′), as previously described[25].

To induce NAFLD, 4-week-old male WT, NR4A1-KO and DNA-PKcs^{LKO} mice were randomly assigned to either a low-fat or high-fat diet for 6 months. The diets used for these studies were commercially available from Research Diets (New Brunswick, NJ, USA). Catalog # D12450B with 10 kcal% fat was used as the control diet and Cat# D12492 was used as the high fat (60 kcal% fat) diet, as our previous study described[26]. Lard was the source of lipid in the high-fat diet. After the first 12 weeks (following confirmation of insulin resistance by glucose tolerance testing), mice were treated with either melatonin (20 mg/kg/day, i.p.) or vehicle control (saline) for 12 weeks while maintaining the mice on their respective low or high-fat diet. Melatonin was initially dissolved in absolute ethanol and then diluted in sterile water to a final concentration of 0.5% ethanol based on our previous study[27, 28].

2.2 | Oral glucose tolerance test (OGTT), blood pressure, insulin, ALT, AST, triglyceride, cholesterol, and leptin measurements

OGTT was performed at the beginning and the end of the treatment period following a 12-h fast, according to our previous study. In brief, mice were fasted for 12 h and were then challenged with glucose (2 g/kg, intraperitoneally). Blood samples were drawn from the tail vein immediately before glucose challenge, as well as 30, 60, 90, and 120 min thereafter. Blood glucose levels were determined using a glucometer.

Serum levels of triglycerides, total cholesterol, adiponectin, aspartate transaminase (AST) and alanine transaminase (ALT) were measured using commercial kits (BioVision, Milpitas, CA, USA) per the manufacturer's protocol. Leptin levels were measured using commercial kits (Millipore, Billerica, MA, USA) per the manufacturer's protocol. Mouse systolic and diastolic blood pressures were measured with a CODA semi-automated non-invasive blood pressure device (Kent Scientific Co, Torrington, CT, USA) as our previous study described[26].

2.3 | Histology and immunofluorescence

Histopathology was analyzed on formalin-fixed paraffin embedded 5- to 6-µm sections stained with hematoxylin and eosin using standard methods and examined via light microscopy.

For immunofluorescence, samples were fixed with 4% paraformaldehyde for 10 min, permeabilized with 0.3% Triton X-100 for 5 min, and blocked with 10% goat serum albumin for 1 h at room temperature. Specimens were subsequently incubated with primary antibodies overnight at 4°C, then washed with PBS three times and incubated with secondary antibody for 45 min at room temperature. The primary antibodies for immunofluorescence staining were as follows: VCAM1 (1:1500, Abcam plc), MMP9 (1:1000, Abcam plc), LC3II (1:1000, Cell Signaling Technology, Inc.). DAPI (Sigma-Aldrich), lysosome stain, (Beyotime, Beijing, China) and a mitochondrion-selective MitoFluor ™ stain (Molecular Probes, Burlington, ONT, CA) were used to label the nuclei, lysosomes, and mitochondria, respectively.

2.4 | Electron microscopy

The ultrastructure of murine livers was evaluated using electron microscopy (Hitachi, Tokyo, Japan). Liver samples were taken at the same site from three mice in each group to prepare slides. Fragments of liver tissues were fixed in 5% glutaraldehyde and 4% paraformaldehyde in 0.1 M sodium cacodylate buffer with 0.05% $CaCl_2$ for 24 h. After washing in 0.1 M sodium cacodylate buffer, tissues were post-fixed in 1% OsO4 and 0.1 M cacodylate buffer overnight, dehydrated and embedded in Embed-812 resin. The sections were stained with 2% uranyl acetate followed by 0.4% lead citrate, and imaged with a Philips 400 electron microscope (Hitachi, Tokyo, Japan).

2.5 | Hepatocyte isolation

The primary hepatocytes were isolated through Hepatocyte Isolation System (Worthington Biochemical Corporation) according to manufacturer's instruction. Tie a loose half-square or equivalent knot around the vein. Locate the vena cava so it can be opened for drainage just before the portal vein. Turn on the perfusion pump containing plain CMF-HBSS with a flow rate 10-15ml/min. Insert the tubing into the portal vein towards the liver. After 7-10 min of CMF-HBSS perfusion,

switch to perfusion with the Enzyme Buffer Solution. Perfuse the liver with the digestion mixture until it swells fully and the liver is fully digested, about 20-30 minutes. At the end of the perfusion, stop the pump, gently place the liver in culture dish, remove the undigested tissue. Subsequently, viable hepatocytes were enriched by percoll gradient centrifugation.

2.6 | ATP Production, mPTP opening and mitochondrial reactive oxygen species (mROS) measurement

Cellular ATP levels were measured using a firefly luciferase-based ATP assay kit (Beyotime, Beijing, China) based on a fluorescence technique as described by our previous study[29]. The opening of the mPTP was visualized by a rapid dissipation of tetramethylrhodamine ethyl ester fluorescence. Arbitrary mPTP opening times were determined as the time when tetramethylrhodamine ethyl ester fluorescence intensity decreased by half between initial and residual fluorescence intensities according to our previous study[30]. The mROS assay was conducted using the MitoSOX red mitochondrial superoxide indicator (Molecular Probes, Burlington, ONT, CA).

2.7 | Mitochondrial membrane potential, cardiolipin oxidation detection and mitochondrial oxygen consumption rate (OCR)

The mitochondrial transmembrane potential was analyzed using a JC-1 Kit (Beyotime, China). Images were captured using a fluorescence microscope (OLYMPUS DX51; Olympus, Tokyo, Japan) and were analyzed with Image-Pro Plus 6.0 software to obtain the mean densities of the region of interest, which were normalized to that of the control group. Staining with 10-N-nonyl acridine orange (NAO; 2 mmol/L, Molecular Probes, Burlington, ONT, CA) was used to detect cardiolipin oxidation.

The mitochondrial oxygen consumption rate (OCR) was evaluated with an XFe96 extracellular flux analyzer (Agilent Technologies, CA, USA). Cells were seeded at 40000 cells/well on 96-well XFe96 cell culture microplates and cultured for 48 h. For respiration assays, cells were incubated in a CO_2-free environment for 1 h, and OCR was measured every 3 min for the next 90 min. First, OCR was quantified in basal conditions (20 mM glucose), then with 1 μM oligomycin (ATP Synthase inhibitor), next with 0.125 μM FCCP (mitochondrial respiration uncoupler), and finally with 1 μM Rotenone/Antimycin A (Complex I and III inhibitors, respectively).

2.8 | qPCR and siRNA

The qPCR assays were carried out as in our previous study. The primers used for polymerase chain reaction were as follows: Bnip3 (forward primer 5'-AAGCAGTTCATCCGCTACCT-3', reverse primer AGACCATCCGTCACCAGATT-3'), TGFβ (forward primer 5'-ACGACATAGACGGCATCCA-3', reverse primer 5'-GCTGTGGTTCAGTTGTGGTG-3'), TNFα (forward primer 5'-ATCCGCGACGTGGAACTG-3', reverse primer 5'-CAGCTCATATGGGTCCGACA-3'), IL-6 (forward primer 5'-CCAGAAACCGCTATGAAGTTCCT-3', reverse primer 5'-CACCAGCATCAGTCCCAAGA-3'). Quantification of gene expression was performed using an ABI PRISM 7500 Sequence Detection System (Applied Biosystems, Foster City, CA, USA). The mRNA levels were determined by qRT-PCR in triplicate for each of the independently prepared RNAs and were normalized to the levels of β-actin expression.

The scrambled siRNA control or siRNA specific against DNA-PKcs, NR4A1, p53 and Bnip3 were purchased from Santa Cruz Biotechnology. For the RNAi knockdown, cells were seeded in plates containing medium without antibiotics for 24 h before transfection. The siRNAs were

transfected into the cells using Lipofectamine 2000 (Invitrogen, Burlington, ONT, CA) in serum-free Opti-MEM (Invitrogen, Burlington, ONT, CA), according to the manufacturer's instructions[31].

2.9 | Western blots

Briefly, cells were lysed on ice for 30 min in radioimmunoprecipitation assay (RIPA) buffer supplemented with the protease inhibitors phenylmethylsulfonyl fluoride (PMSF). Protein samples at a concentration of 50 μg were separated in 8%–15% gradient SDS-PAGE gels and electroblotted onto 0.2-mm nitrocellulose membranes. The membranes were blocked in Tris-buffered saline-Tween (TBS-T; 25 mM Tris, pH 8.0, 150 mM NaCl, and 0.05% Tween-20) containing 5% (w/v) nonfat dried milk for 1 h. After blocking, membranes were probed overnight with primary antibodies. After extensive washings with TBS-T, the blots were incubated with appropriate peroxidase-conjugated secondary antibodies for 1 h at room temperature. Following incubation, the membranes were washed extensively with TBS-T, and detected with a Chemidoc system (Bio-rad, CA, USA). The primary antibodies used in the present study were as follows: LC3II (1:1000, Cell Signaling Technology, Inc., Danvers, MA, USA), Beclin-1 (1:2000, Cell Signaling Technology, Inc., Danvers, MA, USA), Atg5, (1:2000, Abcam plc, Cambridge, MA, USA), Drp1 (1:1000, Cell Signaling Technology, Inc.,

Danvers, MA, USA), p53 (1:1000, Cell Signaling Technology, Inc., Danvers, MA, USA), p53 (Ser15) (1:1000, Cell Signaling Technology, Inc., Danvers, MA, USA), DNA-PKcs (1:1000, Abcam plc, Cambridge, MA, USA), NR4A1 (1:1000, Abcam plc, Cambridge, MA, USA), Bnip3 (1:1000, Cell Signaling Technology, Inc., Danvers, MA, USA).

2.10 | Reagent treatment

To mimic the high-fat injury in vitro, palmitic acid (PA, 75 μM, Selleck Chemicals, Houston, TX, USA) was added to the primary hepatocyte culture for approximately 24 h. For melatonin protection, 100 μmol/L melatonin was used in the presence or absence of PA for approximately 24 h. To activate NR4A1, cytosporone B (CsnB, 10 μg/ml, Selleck Chemicals, Houston, TX, USA) was used 4 h prior to melatonin treatment. To knockdown the expression of NR4A1, DNA-PKcs, p53 and Bnip3, siRNAs against NR4A1, DNA-PKcs, p53 and Bnip3 were used before PA treatment. To activate mitochondrial fission, 5 μM FCCP (Selleck Chemicals, Houston, TX, USA) was added to the medium for 4 h prior to PA treatment.

2.11 | Statistical Analysis

GraphPad Prism 6.0 for Windows software (GraphPad Software, San Diego, CA, USA) was used for all statistical calculations. All data are presented as the means and standard error. The data were analyzed using one-way analysis of variance (ANOVA). $P<0.05$ was considered statistically significant.

3 | RESULTS

3.1 | NR4A1 abolition prevents the diet-induced NAFLD

We first observed changes in NR4A1 levels in mice fed a low-fat diet (LFD) or high-fat diet (HFD). Compared to the LFD group, the liver NR4A1 expression was increased in response to the HFD treatment (Figure 1A-B). However, melatonin ameliorated the increased NR4A1 level in HFD mice. To determine the role of NR4A1 in NAFLD, NR4A1 genetically deleted (NR4A1-KO) mice were used. The general characteristics of NR4A1-KO mice fed a HFD or LFD were analyzed. As shown in Supplemental Table, the HFD was associated with increased body and liver weights compared to the LFD group; these effects were attenuated by NR4A1 genetic ablation or melatonin treatment (food

intake was comparable among all mouse groups regardless of diet or treatment). Moreover, mice receiving the HFD had a higher caloric intake, which was surprisingly attenuated in both the melatonin-treated mice and the NR4A1-KO mice. However, the systolic and diastolic blood pressures were comparable among all mouse groups regardless of diet or treatment. The blood glucose level was also increased in the HFD group but was reduced in the melatonin-treated mice or NR4A1-KO mice.

Following oral glucose challenge, the HFD treatment impaired the glucose clearance ability compared to mice fed with LFD (Figure 1C). Although melatonin failed to alter the post-challenge glucose levels in HFD-treated mice, it had a small yet significant glucose lowering effect at 60 and 120 min post-glucose challenge. In contrast, knockdown of NR4A1 could restore the glucose levels to normal. Additional markers of liver damage, such as the triglycerides, total cholesterol, aspartate transaminase (AST) and alanine transaminase (ALT), adiponectin and leptin levels, were all elevated in the HFD mice but reduced in the melatonin-treated mice or NR4A1-KO mice (Figure 1D-I).

3.2 | Melatonin attenuates hepatic lipogenesis and fibrosis via inhibition of NR4A1

To assess the roles of melatonin and NR4A1 in the etiology of NAFLD, we next examined histological changes in the liver. WT mice developed severe NAFLD with HFD treatment, as shown by the presence of hepatocyte vacuolation, steatosis, and fibrosis (Figure 2A-D). Strikingly, these defects were completely absent in the livers of NR4A1-KO mice or mice treated with melatonin.

Additionally, we used electron microscopy (EM) to observe the ultrastructural changes in the liver. Compared to the LFD-treated mice, the HFD induced lipid accumulation and mitochondrial dysfunction (mitochondria with the abnormal appearance such as swell, disorganization and reduction or vanish of the crista in the amplified panel). However, knockdown of NR4A1 or treatment with melatonin had the ability to reverse such changes (Figure 2A).

Moreover, we performed immunofluorescence to evaluate inflammatory markers during the development of NAFLD. Compared to the LFD-treated mice, the HFD augmented the expression of matrix metallopeptidase 9 (MMP9) and vascular cell adhesion protein 1 (VCAM1) (Figure 2E). Moreover, the PCR assays also indicated that more transcriptions of interleukin 6 (IL-6), tumor necrosis factor α (TNFα) and transforming growth factor β (TGFβ) appeared in the HFD-treated mice (Figure 2F-H). However, NR4A1 deficiency or melatonin treatment alleviated the expression (Figure

2E) and transcriptions (Figure 2F-H) of these inflammatory markers. Taken together, these data exhibit that NR4A1 plays an important role in the progression of NAFLD and that melatonin maintains normal liver structure and function by abrogating the effects of NR4A1.

3.3 | NR4A1 activates Drp1-related mitochondrial fission

Mitochondrial dysfunction is putatively implicated in the pathogenesis of NAFLD and an important determinant of mitochondrial function is mitochondrial fission[32]. Thus, we observed the morphological changes of mitochondria under palmitic acid treatment (PA, 75 μM for 24 h), which was used to mimic high-fat injury in hepatocyte. Then, the mitochondrial length was examined to quantify mitochondrial fission. In control cells, the mitochondria were funicular and the length of the mitochondria was 7.9 ± 1.8 mm (Figure 3A-B). However, in the PA-treated cells, the mitochondria were divided into several fragments and the length was reduced to 2.3 ± 0.8 mm. However, melatonin-treated cells or NR4A1-deleted cells showed predominantly elongated forms of mitochondria despite treatment with PA. Intriguingly, activation of NR4A1 by cytosporone B (CsnB) negated the protective effect of melatonin on mitochondrial fission (Figure 3A-B).

Drp1 transport to mitochondria is a prerequisite for mitochondrial fission. In Figure 3C-E, PA increased mito-Drp1 expression but reduced cyto-Drp1 content. These tendencies were reversed by NR4A1 deletion or melatonin treatment. Notably, activation of NR4A1 by CnsB cancelled the inhibitory effect of melatonin on Drp1 migration. To provide more robust evidence for the role of NR4A1 in Drp1-related fission, we performed co-immunofluorescence of mitochondria and Drp1 to observe the Drp1 cellular localization and mitochondrial debris simultaneously. As shown in Figure 3F, the control cells exhibited spindle mitochondria with no Drp1 accumulation. In contrast, PA treatment produced massive mitochondrial fragmentations that were marked by Drp1. However, loss of NR4A1 could alleviate the number of mitochondrial fragmentations and separate the Drp1 away from the mitochondria, similar to the data in melatonin-treated cells. Notably, once reactivation of NR4A1, the beneficial influence of melatonin on fission disappeared (Figure 3F). Altogether, these results hint that melatonin inactivates Drp1-related mitochondrial fission via NR4A1.

3.4 | Melatonin reduces cellular oxidative stress and calcium overload via suppressing fission

Next, to tease out the consequence of fission inhibition by melatonin, we evaluated the mitochondrial function. PA elevated the mitochondrial ROS (mROS) production (Figure 4A-B) and mPTP opening rate (Figure 4C). However, these changes were reversed by melatonin treatment. Notably,

re-activation of fission via FCCP limited the protective effects of melatonin on mPTP opening and mROS clearing.

As a consequence of mitochondrial oxidative stress, more cardiolipin was oxidized by PA via NAO staining assay[33]. However, melatonin alleviated the mitochondrial lipid oxidation via inhibition of NR4A1 and fission (Figure 4D-E). Furthermore, PA also reduced the GSH and SOD levels but increased MDA concentration (Figure 4F-H). Whereas melatonin treatment restored the levels of antioxidant factors and decreased MDA generation. However, the anti-oxidant activity of melatonin was nullified by fission activator FCCP (Figure 4F-H).

Additionally, mitochondria are the second calcium pool which shape cellular Ca^{2+} signals by acting as a Ca^{2+} buffer and releasing Ca^{2+} into cytoplasm[34]. We used a calcium map to quantify the cytoplasmic calcium alterations during mitochondrial fission. After exposure to PA, the calcium intensity was increased, indicative of calcium overload (Figure 4I-J). However, application of melatonin to modulate NR4A1-mediated mitochondrial fission repressed the calcium fluctuation. Altogether, these data illustrate that NR4A1 induces mitochondrial malfunction via Drp1-related mitochondrial fission, which is abolished by melatonin.

3.5 | NR4A1 represses Bnip3-required mitophagy

Apart from mitochondrial fission, mitophagy is another catabolic process involving degradation of unnecessary or dysfunctional mitochondria by lysosomes. For Bnip3-required mitophagy, few references exist describing its role in NAFLD, although several studies have hinted that Bnip3 deficiency aggravates insulin resistance and metabolic syndrome[35]. Based on these, we explored the role of Bnip3-related mitophagy in NAFLD. First, we found Bnip3 expression was reduced in response to PA stimulation (Figure 5A-B), and this change was due to its downregulated mRNA transcription (Figure 5C). However, melatonin treatment or NR4A1 knockdown could reverse Bnip3 transcription and expression. Notably, reintroduction of NR4A1 by CsnB limited the promotive effect of melatonin on Bnip3 expression regardless of at mRNA or protein levels.

Next, to observe the role of melatonin in Bnip3-required mitophagy, mitochondria and lysosome co-staining was used. The control cells exhibited spindle mitochondria with distributed lysosomes (Figure 5D). However, after PA treatment, the mitochondrial morphology became small, with roundish fragments that are characteristic of fission. Moreover, these mitochondrial debris were not tagged with lysosomes, suggestive of mitophagy inhibition (Figure 5D). In contrast, NR4A1 deficiency or melatonin treatment led to small and roundish mitochondria that were engulfed by

lysosomes, thereby restoring mitochondrial networks and suggesting mitophagy activation. However, re-activation of NR4A1 by CnsB or silence of Bnip3 via siRNA abrogated the promotional effect of melatonin on mitophagy.

Next, to quantify mitophagy, we used western blots to detect the markers of mitophagy such as Atg5, Beclin1 and mito-LC3II. There parameters were decreased after PA treatment but increased under melatonin treatment (Figure 5E-G). In contrast, CnsB treatment or Bnip3 knockdown also reduced the expression of mitophagy markers in melatonin-treated cells. At last, autophagic flux measurement was carried out to further demonstrate the role of melatonin on Bnip3-required mitophagy. LC3II accumulation to the mitochondria was repressed by PA but enhanced by NR4A1 deficiency or melatonin treatment (Figure 5H). However, melatonin's effect was cancelled by CsnB application or Bnip3 knockdown. Altogether, these data indicate that NR4A1 limits Bnip3-required mitophagy which is sustained by melatonin.

3.6 | Melatonin protects mitochondrial respiratory function via improving mitophagy

In light of the central role of mitochondria in ATP production[36], we examined the energy production under Bnip3-required mitophagy. As expected, PA abated the ATP production (Figure 6A); however, melatonin application could improve the ATP generation. After knockdown of Bnip3, the melatonin-mediated ATP production was reduced. The ATP is actually derived from the proton chemical gradient that forms the mitochondrial inner membrane potential ($\Delta\Psi m$)[37, 38]. We found that the $\Delta\Psi m$ was dissipated in response to PA insult (Figure 6B-C). However, melatonin rescued the $\Delta\Psi m$ dissipation in a Bnip3-dependent manner.

Next, we used the oxygen consumption rate (OCR) assay to observe mitochondrial respiratory function. The OCR was decreased after PA treatment (Figure 6D). However, melatonin supplementation, could restore the OCR in primary hepatocytes via upregulation of Bnip3. Moreover, compared with control cells, basal respiration rates were significantly decreased with PA treatment but increased after melatonin treatment (Figure 6E). Furthermore, proton leaking, maximal respiratory capacity and ATP turnover were significantly reduced in PA-treated cells compared with the control group (Figure 6F-H). However, melatonin application improved the mitochondrial respiratory parameters in PA-treated cells via improvement of Bnip3.

3.7 | NR4A1 modulates Drp1 and Bnip3 via DNA-PKcs/p53 pathway

At last, to explore the mechanism by which NR4A1 regulated Drp1 migration and Bnip3 transcription, we focused on p53. Firstly, phosphorylated p53 was increased under PA treatment but decreased after loss of NR4A1 or treatment with melatonin (Figure 7A-B). To demonstrate whether p53 was involved in fission and mitophagy regulation, we examined the Drp1 cellular compartmentalization and Bnip3 expression. In PA-treated cells, silence of p53 abated the mito-Drp1 content but reversed the cyto-Drp1 expression (Figure 7A and C), which was similar to the results of melatonin treatment. Besides, knockdown of p53 also rescued the Bnip3 expression under PA treatment (Figure 7A and D). These data clarify the causal role of p53 in Drp1 and Bnip3 modulation.

Recent study has identified DNA-PKcs as the bridge connecting upstream NR4A1 and downstream p53 in liver cancer[12]. In the current study, we found that DNA-PKcs was upregulated by PA treatment (Figure 7E-F), but reduced in NR4A1-deleted or melatonin-treated cells. Next, silence of DNA-PKcs, the p53 phosphorylation was declined (Figure 7E). Altogether, these data propose that DNA-PKcs/p53 activation is depended on NR4A1, and that melatonin could inactivate NR4A1/DNA-PKcs/p53 pathway to inhibit Drp1 translocation and sustain Bnip3 activity.

To more specifically characterize the effects of DNA-PKcs in mitochondrial fission and mitophagy, we measured the mitochondrial length and mitophagy markers. Silence of DNA-PKcs preserved the mitophagy markers (Figure 7E, G-H) and restored the mitochondrial length (Figure 7I). These data were comparable to the results from the NR4A1-knockout cells and melatonin-treated cells.

At last, to provide more evidences for the role of DNA-PKcs in the development of NAFLD, we subjected hepatocyte-specific DNA-PKcs knockout mice to HFD stimulation. As shown in Figure 7J-L, compared to the mice fed a LFD, the HFD induced hepatocyte vacuolation and augmented the number of TUNEL-positive cells. However, genetic ablation of DNA-PKcs in the liver blocked this phenotype; these data are comparable to the results from the NR4A1-knockout mice and melatonin-treated mice. Collectively, the above findings underscore the inductive role of DNA-PKcs in the mitochondrial homeostasis. At the molecular level, DNA-PKcs is regulated by NR4A1 and signals p53 to evoke Drp1-related fission and repress Bnip3-required mitophagy, whereas melatonin has the ability to inhibit NR4A1/DNA-PKcs/p53 pathway and manipulate mitochondrial homeostasis.

4 | DISCUSSION

Ample evidence suggests the involvement of melatonin in the protection of liver function in diabetes, high-fat diet[39], liver fibrosis[40], and hepatocellular carcinoma[41]. However, little is known about the role of melatonin in the repair of non-alcoholic fatty liver disease (NAFLD). In the present study, we found that (1) melatonin largely reversed the pathogenesis of HFD-induced NAFLD by improving mitochondrial function via inhibition of the NR4A1/DNA-PKcs/p53 pathway, (2) NR4A1 was highly dysregulated in the development of NAFLD and contributed to DNA-PKcs elevation and p53 activation, (3) p53 activation via phosphorylation at Ser15 launched Drp1-induced mitochondrial fission but blunted Bnip3-required mitophagy, (4) mitochondrial fission evoked cellular oxidative injury and calcium overload, (5) defective mitophagy impaired mitochondrial energy production, and (6) melatonin attenuated mitochondrial fission and reversed the reduction in mitophagy, protecting mitochondrial homeostasis in NAFLD. To the best of our knowledge, this is the first study to comprehensively describe the crucial and complicated role of melatonin in the development of NAFLD involving the NR4A1/DNA-PKcs/p53 pathway, mitochondrial division and mitophagy (Fig. 8).

The hallmark histological feature of NAFLD is the accumulation of fat in hepatocytes[42]. Furthermore, the consequential surplus of lipids in hepatocytes results in oxidative stress and lipotoxicity[43], and promotes mitochondrial dysfunction via a variety of intra- and inter-cellular signaling mechanisms[44]. Mitochondrial damage results in hepatocyte death or dysfunction[45]. With the loss of functional liver tissue, hepatic stellate cells are activated and contribute to the accumulation of extracellular matrix proteins, leading to fibrosis[46]. Thus, protection of mitochondria against lipotoxicity is vital to retard or reverse the progression of NAFLD.

Ample evidences have indicated that melatonin could reduce hepatocytes injury via multiple mechanisms. Melatonin treatment attenuates hepatic oxidative stress[47], increases the expression of anti-oxidant factor such as GSH, alleviates the hepatic endoplasmic reticulum (ER) stress[48], sustains cellular calcium homeostasis via regulation of micro-RNA[49] and inhibits MAPK-JNK/P38-induced hepatocytes death[50]. Importantly, more clinical evidences have confirmed the effective role of melatonin in treating patients with NAFLD[51, 52, 53, 54]. Therefore, supplementation of melatonin would bring more clinical benefits to patients suffered from NAFLD. In the present study, we found that melatonin diminished the risk of NAFLD via protection of mitochondria. Mechanistically, melatonin reversed the loss of mitochondrial respiratory function, cut off the cellular oxidative injury and

alleviated the calcium overload under high-fat stimulation. Furthermore, two types of molecular mechanisms account for the protective role of melatonin in mitochondria: reducing mitochondrial fission and promoting mitophagy.

Moderate mitochondrial fission actively helps the mitochondrial networks to communicate with each other. However, excessive fission can critically impair the mitochondrial genome according to our previous work, leading to the damage of mtDNA that encodes 13 polypeptides involved in oxidative phosphorylation and mitochondrial structure[30]. In the present study, we found that fission caused mPTP opening, which was accompanied by increased mROS generation. This change upset the redox balance, resulting into the overconsumption of antioxidant factors, a key feature of cellular oxidative injury. Moreover, fission also evoked calcium overload, which is the decisive element for cellular dysfunction. The mechanism underlying fission-mediated calcium overload may be attributed to mitochondrial calcium leakage and the ATP shortage. One possibility is that the mPTP opening provides a channel for the mitochondria-contained calcium to be released into the cytoplasm. Second, cytoplasm calcium recycling is an ATP-dependent process dependent on the sarcoplasmic reticulum Ca^{2+} ATPase (SERCA)[55]. Based on our previous report[29], the decline in ATP concentration would

inactivate SERCA, leading to its failure to recycle cytoplasmic calcium back into the endoplasmic reticulum and/or sarcoplasmic reticulum.

As for mitophagy, three kinds of receptors (FUNDC1, Parkin and Bnip3) have been found to be involved in mitophagy. In liver fibrosis, mitophagy activation is a protective system activated by melatonin[40]. Interestingly, in the late stages of liver fibrosis, such as hepatocellular carcinoma, mitophagy activation by melatonin augments cancer cell death[56]. Our team has performed significant research concerning mitophagy, and based on our previous study, autophagy activation in alcohol-induced hepatic steatosis would ameliorate liver damage[57]. Moreover, FUNDC1-required mitophagy activation also confers protection against reperfusion injury[37]. In contrast, Parkin-related mitophagy activation can aggravate cellular damage[28]. These conflicting results highlight that the mitophagy receptor determines the mitophagy function, ranging from cellular protection to cellular self-destruction. In the present study, we focused on Bnip3-required mitophagy, because no research is currently available regarding its role in NAFLD. We found that Bnip3-required mitophagy was necessary for mitochondrial protection via improvement of ATP production and mitochondrial respiration. These data put forward that Bnip3-required mitophagy could be considered as a potential target for therapeutic intervention against the development of NAFLD. In agreement with these

findings, previous studies found that upregulation of Bnip3 maintained mitochondrial integrity and ameliorated liver fibrosis in the diabetic liver[35, 58].

We determined that NR4A1/DNA-PKcs/p53 signaling encodes a damage signal for fission activation and mitophagy inhibition, which could be abolished by melatonin. NR4A1 acts primarily as a transcription factor to regulate the expression of multiple genes. However, increasing research attention has recently been focused on nongenomic activities of NR4A1. Our current study described its role in DNA-PKcs activation[12]. DNA-PKcs, a family of phosphatidylinositol 3-kinase-like kinases, is a central enzyme involved in DNA repair for mammalian cells[13]. Many DNA-PKcs substrates have been identified, including Ku70, Ku80 and p53. Ku80 can recognize and bind to the broken ends of double-stranded DNA, which is responsible for DNA-repair[14]. Therefore, this pathway functions as an intrinsic repair signal to promote cellular survival. Another substrate, p53, could be phosphorylated by DNA-PKcs at Ser15[12]. The phosphorylated p53 is more stable when compared to the nonphosphorylated p53, and can initiate cellular suicide procedures. Thus, the DNA-PKcs/p53 is consider as a cellular self-clearing system functioning in response to prolonged insult or irreparable cell damage. In the present study, hyper-activated NR4A1 preferentially drove the DNA-PKcs/p53 signaling, leading to mitochondrial dysfunction in the development of NAFLD.

On the one hand, NR4A1/DNA-PKcs/p53 pathway assisted Drp1 migration onto the surface of mitochondria, forcing mitochondrial fission. Because Drp1 is usually a cytoplasmic protein, its relocation on the surface requires a receptor. Several receptors have been identified, such as Mff and Fis1[30]; p53 has also been reported to be involved in Drp1 translocation onto the mitochondria. On the other hand, NR4A1/DNA-PKcs/p53 pathway was a functionally transcriptional repressor of Bnip3[59], which mediated mitophagy impairment. The p53 could directly bind to a p53-response element motif and recruit the corepressor mSin3a to the Bnip3 promoter in zebrafish[59]. This may be the underlying mechanism responsible for the inhibitory action of NR4A1/DNA-PKcs/p53 pathway on Bnip3 expression. These results define NR4A1/DNA-PKcs/p53 pathway as the convergent upstream signals for mitochondrial fission and mitophagy in response to NAFLD for the first time. Meanwhile, we also confirm that melatonin has the ability to cut off the NR4A1/DNA-PKcs/p53 pathway, which confers a protective advantage to mitochondria via balancing Drp1-related fission and Bnip3-required mitophagy. Notably, other factors are also associated with the mitochondrial homeostasis including toll-like receptor 4 (TLR4)[60], PINK1/Parkin[61], RORα[62], SIRT3[63]. Whether these factors are related to the protective role of melatonin in liver and mitochondrial injury remains unclear. More researches are needed to support this notion. Altogether, our conclusions provide solid evidence supporting

melatonin supplementation in the treatment of NAFLD. This would be especially valid since NAFLD typically occurs in older individuals whose endogenous melatonin levels are very low.

There are a few limitations to our study. First, the loss-of NR4A1 function experiments were performed in global NR4A1 knockout mice, which could influence the NR4A1 expression throughout the body. Therefore, liver-specific NR4A1-knockout mice will be needed in the future to further validate our findings. A second limitation of our study is that pharmacological agent of NR4A1 could bring some sides effects. Meanwhile, we did not conduct the gain-of function assay about NR4A1 in vivo. Accordingly, the transgenic mice of NR4A1 with melatonin treatment would bring more direct and solid evidence to explain the regulatory role of melatonin in NR4A1-related NAFLD.

ACKNOWLEDGEMENTS

This study was supported by grants from the National Natural Science Foundation of China (No. 81770237) and the science technological innovation nursery fund of People Liberation Army General Hospital (No. 16KMZ02). The funders had no role in the study design, data collection and analysis, decision to publish, or preparation of the manuscript.

DISCLOSURE

The authors have declared that they have no conflicts of interest.

AUTHOR CONTRIBUTIONS

HZ, WHW and JR involved in conception and design, performance of experiments, data analysis and interpretation, and manuscript writing; WJD, NH, and SM involved in the development of methodology, CS and YL involved in the data acquisition, HZ and CS involved data analysis and interpretation; HZ and WHW involved in study supervision and final approval of manuscript.

References

1. Grundy SM. Metabolic syndrome update. *Trends Cardiovasc Med.* 2016;26:364-373.

2. Bellanti F, Villani R, Facciorusso A, et al. Lipid oxidation products in the pathogenesis of non-alcoholic steatohepatitis. *Free Radic Biol Med.* 2017;111:173-185.

3. Italian Association for the Study of the L. AISF position paper on nonalcoholic fatty liver disease (NAFLD): Updates and future directions. *Dig Liver Dis.* 2017;49:471-483.

4. Younossi ZM, Blissett D, Blissett R, et al. The economic and clinical burden of nonalcoholic fatty liver disease in the United States and Europe. *Hepatology.* 2016;64:1577-1586.

5. Bingol B, Sheng M. Mechanisms of mitophagy: PINK1, Parkin, USP30 and beyond. *Free Radic Biol Med.* 2016;100:210-222.

6. Quijano C, Trujillo M, Castro L, et al. Interplay between oxidant species and energy metabolism. *Redox Biol.* 2016;8:28-42.

7. Rodney GG, Pal R, Abo-Zahrah R. Redox regulation of autophagy in skeletal muscle. *Free Radic Biol Med.* 2016;98:103-112.

8. Dashzeveg N, Yoshida K. Cell death decision by p53 via control of the mitochondrial membrane. *Cancer Lett.* 2015;367:108-112.

9. Ni HM, Williams JA, Ding WX. Mitochondrial dynamics and mitochondrial quality control. *Redox Biol.* 2015;4:6-13.

10. Wang EY, Gang H, Aviv Y, et al. p53 mediates autophagy and cell death by a mechanism contingent on Bnip3. *Hypertension.* 2013;62:70-77.

11. Carrasco-Pozo C, Tan KN, Reyes-Farias M, et al. The deleterious effect of cholesterol and protection by quercetin on mitochondrial bioenergetics of pancreatic beta-cells, glycemic control and inflammation: In vitro and in vivo studies. *Redox Biol.* 2016;9:229-243.

12. Zhao BX, Chen HZ, Du XD, et al. Orphan receptor TR3 enhances p53 transactivation and represses DNA double-strand break repair in hepatoma cells under ionizing radiation. *Mol Endocrinol.* 2011;25:1337-1350.

13. Kai M. Roles of RNA-binding proteins in DNA damage response. *Int J Mol Sci.* 2016;17:310.

14. Woods DS, Sears CR, Turchi JJ. Recognition of DNA termini by the C-terminal region of the Ku80 and the DNA-dependent protein kinase catalytic subunit. *PLoS One.* 2015;10:e0127321.

15. Pawlak A, Strzadala L, Kalas W. Non-genomic effects of the NR4A1/Nur77/TR3/NGFIB orphan nuclear receptor. *Steroids.* 2015;95:1-6.

16. Krishnamurthy B, Chee J, Jhala G, et al. BIM deficiency protects NOD mice from diabetes by diverting thymocytes to regulatory T cells. *Diabetes.* 2015;64:3229-3238.

17. Chen Y, Wu R, Chen HZ, et al. Enhancement of hypothalamic STAT3 acetylation by nuclear receptor Nur77 dictates leptin sensitivity. *Diabetes.* 2015;64:2069-2081.

18. Kolluri SK, Zhu X, Zhou X, et al. A short Nur77-derived peptide converts Bcl-2 from a protector to a killer. *Cancer Cell.* 2008;14:285-298.

19. Tan DX, Hardeland R, Back K, et al. On the significance of an alternate pathway of melatonin synthesis via 5-methoxytryptamine: comparisons across species. *J Pineal Res.* 2016;61:27-40.

20. de Luxan-Delgado B, Potes Y, Rubio-Gonzalez A, et al. Melatonin reduces endoplasmic reticulum stress and autophagy in liver of leptin-deficient mice. *J Pineal Res.* 2016;61:108-123.

21. Winiarska K, Dzik JM, Labudda M, et al. Melatonin nephroprotective action in Zucker diabetic fatty rats involves its inhibitory effect on NADPH oxidase. *J Pineal Res.* 2016;60:109-117.

22. Xu S, Pi H, Zhang L, et al. Melatonin prevents abnormal mitochondrial dynamics resulting from the neurotoxicity of cadmium by blocking calcium-dependent translocation of Drp1 to the mitochondria. *J Pineal Res.* 2016;60:291-302.

23. Chen HH, Chen YT, Yang CC, et al. Melatonin pretreatment enhances the therapeutic effects of exogenous mitochondria against hepatic ischemia-reperfusion injury in rats through suppression of mitochondrial permeability transition. *J Pineal Res.* 2016;61:52-68.

24. Kleszczynski K, Zillikens D, Fischer TW. Melatonin enhances mitochondrial ATP synthesis, reduces reactive oxygen species formation, and mediates translocation of the nuclear erythroid 2-related factor 2 resulting in activation of phase-2 antioxidant enzymes (gamma-GCS, HO-1, NQO1) in ultraviolet radiation-treated normal human epidermal keratinocytes (NHEK). *J Pineal Res.* 2016;61:187-197.

25. Mishra A, Brown AL, Yao X, et al. Dendritic cells induce Th2-mediated airway inflammatory responses to house dust mite via DNA-dependent protein kinase. *Nat Commun.* 2015;6:6224.

26. Ceylan-Isik AF, Kandadi MR, Xu X, et al. Apelin administration ameliorates high fat diet-induced cardiac hypertrophy and contractile dysfunction. *J Mol Cell Cardiol.* 2013;63:4-13.

27. Zhou H, Li D, Zhu P, et al. Melatonin suppresses platelet activation and function against cardiac ischemia/reperfusion injury via PPARgamma/FUNDC1/mitophagy pathways. *J Pineal Res.* 2017;e12438.

28. Zhou H, Zhang Y, Hu S, et al. Melatonin protects cardiac microvasculature against ischemia/reperfusion injury via suppression of mitochondrial fission-VDAC1-HK2-mPTP-mitophagy axis. *J Pineal Res.* 2017;63:e12413.

29. Zhang Y, Zhou H, Wu W, et al. Liraglutide protects cardiac microvascular endothelial cells against hypoxia/reoxygenation injury through the suppression of the SR-Ca(2+)-XO-ROS axis via activation of the GLP-1R/PI3K/Akt/survivin pathways. *Free Radic Biol Med.* 2016;95:278-292.

30. Zhou H, Hu S, Jin Q, et al. Mff-dependent mitochondrial fission contributes to the pathogenesis of cardiac microvasculature ischemia/reperfusion injury via induction of

mROS-mediated cardiolipin oxidation and HK2/VDAC1 disassociation-involved mPTP opening. *J Am Heart Assoc.* 2017;6:e005328.

31. Zhou H, Yang J, Xin T, et al. Exendin-4 enhances the migration of adipose-derived stem cells to neonatal rat ventricular cardiomyocyte-derived conditioned medium via the phosphoinositide 3-kinase/Akt-stromal cell-derived factor-1alpha/CXC chemokine receptor 4 pathway. *Mol Med Rep.* 2015;11:4063-4072.

32. Du K, Ramachandran A, Jaeschke H. Oxidative stress during acetaminophen hepatotoxicity: Sources, pathophysiological role and therapeutic potential. *Redox Biol.* 2016;10:148-156.

33. Reiter RJ, Mayo JC, Tan DX, et al. Melatonin as an antioxidant: under promises but over delivers. *J Pineal Res.* 2016;61:253-278.

34. King AL, Mantena SK, Andringa KK, et al. The methyl donor S-adenosylmethionine prevents liver hypoxia and dysregulation of mitochondrial bioenergetic function in a rat model of alcohol-induced fatty liver disease. *Redox Biol.* 2016;9:188-197.

35. Tol MJ, Ottenhoff R, van Eijk M, et al. A PPARgamma-bnip3 axis couples adipose mitochondrial fusion-fission balance to systemic insulin sensitivity. *Diabetes.* 2016;65:2591-2605.

36. Kozlov AV, Lancaster JR, Jr., Meszaros AT, et al. Mitochondria-meditated pathways of organ failure upon inflammation. *Redox Biol.* 2017;13:170-181.

37. Zhou H, Zhu P, Guo J, et al. Ripk3 induces mitochondrial apoptosis via inhibition of FUNDC1 mitophagy in cardiac IR injury. *Redox Biol.* 2017;13:498-507.

38. Fuhrmann DC, Brune B. Mitochondrial composition and function under the control of hypoxia. *Redox Biol.* 2017;12:208-215.

39. Das N, Mandala A, Naaz S, et al. Melatonin protects against lipid-induced mitochondrial dysfunction in hepatocytes and inhibits stellate cell activation during hepatic fibrosis in mice. *J Pineal Res.* 2017;62:e12404.

40. Kang JW, Hong JM, Lee SM. Melatonin enhances mitophagy and mitochondrial biogenesis in rats with carbon tetrachloride-induced liver fibrosis. *J Pineal Res.* 2016;60:383-393.

41. Lin S, Hoffmann K, Gao C, et al. Melatonin promotes sorafenib-induced apoptosis through synergistic activation of JNK/c-jun pathway in human hepatocellular carcinoma. *J Pineal Res.* 2017;62:e12398.

42. Younossi ZM, Koenig AB, Abdelatif D, et al. Global epidemiology of nonalcoholic fatty liver disease-Meta-analytic assessment of prevalence, incidence, and outcomes. *Hepatology.* 2016;64:73-84.

43. Kakimoto PA, Kowaltowski AJ. Effects of high fat diets on rodent liver bioenergetics and oxidative imbalance. *Redox Biol.* 2016;8:216-225.

44. Wong RJ, Aguilar M, Cheung R, et al. Nonalcoholic steatohepatitis is the second leading etiology of liver disease among adults awaiting liver transplantation in the United States. *Gastroenterology.* 2015;148:547-555.

45. Mailloux RJ, Craig Ayre D, Christian SL. Induction of mitochondrial reactive oxygen species production by GSH mediated S-glutathionylation of 2-oxoglutarate dehydrogenase. *Redox Biol.* 2016;8:285-297.

46. Kheradpezhouh E, Barritt GJ, Rychkov GY. Curcumin inhibits activation of TRPM2 channels in rat hepatocytes. *Redox Biol.* 2016;7:1-7.

47. Hatzis G, Ziakas P, Kavantzas N, et al. Melatonin attenuates high fat diet-induced fatty liver disease in rats. *World J Hepatol.* 2013;5:160-169.

48. Fernandez A, Ordonez R, Reiter RJ, et al. Melatonin and endoplasmic reticulum stress: relation to autophagy and apoptosis. *J Pineal Res.* 2015;59:292-307.

49. Kim SJ, Kang HS, Lee JH, et al. Melatonin ameliorates ER stress-mediated hepatic steatosis through miR-23a in the liver. *Biochem Biophys Res Commun.* 2015;458:462-469.

50. Sun H, Wang X, Chen J, et al. Melatonin improves non-alcoholic fatty liver disease via MAPK-JNK/P38 signaling in high-fat-diet-induced obese mice. *Lipids Health Dis.* 2016;15:202.

51. Pakravan H, Ahmadian M, Fani A, et al. The effects of melatonin in patients with nonalcoholic fatty liver disease: a randomized controlled trial. *Adv Biomed Res.* 2017;6:40.

52. Celinski K, Konturek PC, Slomka M, et al. Effects of treatment with melatonin and tryptophan on liver enzymes, parameters of fat metabolism and plasma levels of cytokines in patients with non-alcoholic fatty liver disease--14 months follow up. *J Physiol Pharmacol.* 2014;65:75-82.

53. Gonciarz M, Gonciarz Z, Bielanski W, et al. The pilot study of 3-month course of melatonin treatment of patients with nonalcoholic steatohepatitis: effect on plasma levels of liver enzymes, lipids and melatonin. *J Physiol Pharmacol.* 2010;61:705-710.

54. Reagan-Shaw S, Nihal M, Ahmad N. Dose translation from animal to human studies revisited. *FASEB J.* 2008;22:659-661.

55. Zhu H, Jin Q, Li Y, et al. Melatonin protected cardiac microvascular endothelial cells against oxidative stress injury via suppression of IP3R-[Ca2+]c/VDAC-[Ca2+]m axis by activation of MAPK/ERK signaling pathway. *Cell Stress Chaperones.* 2017. doi: 10.1007/s12192-017-0827-4.

56. Prieto-Dominguez N, Ordonez R, Fernandez A, et al. Melatonin-induced increase in sensitivity of human hepatocellular carcinoma cells to sorafenib is associated with reactive oxygen species production and mitophagy. *J Pineal Res.* 2016;61:396-407.

57. Guo R, Xu X, Babcock SA, et al. Aldehyde dedydrogenase-2 plays a beneficial role in ameliorating chronic alcohol-induced hepatic steatosis and inflammation through regulation of autophagy. *J Hepatol.* 2015;62:647-656.

58. Glick D, Zhang W, Beaton M, et al. BNip3 regulates mitochondrial function and lipid metabolism in the liver. *Mol Cell Biol.* 2012;32:2570-2584.

59. Feng X, Liu X, Zhang W, et al. p53 directly suppresses BNIP3 expression to protect against hypoxia-induced cell death. *EMBO J.* 2011;30:3397-3415.

60. Nduhirabandi F, Lamont K, Albertyn Z, et al. Role of toll-like receptor 4 in melatonin-induced cardioprotection. *J Pineal Res.* 2016;60:39-47.

61. Diaz-Casado ME, Lima E, Garcia JA, et al. Melatonin rescues zebrafish embryos from the parkinsonian phenotype restoring the parkin/PINK1/DJ-1/MUL1 network. *J Pineal Res.* 2016;61:96-107.

62. He B, Zhao Y, Xu L, et al. The nuclear melatonin receptor RORalpha is a novel endogenous defender against myocardial ischemia/reperfusion injury. *J Pineal Res.* 2016;60:313-326.

63. Zhai M, Li B, Duan W, et al. Melatonin ameliorates myocardial ischemia reperfusion injury through SIRT3-dependent regulation of oxidative stress and apoptosis. *J Pineal Res.* 2017;63:12419.

FIGURE LEGENDS

FIGURE 1

NR4A1 was upregulated in liver tissue and contributed to the development of NAFLD. (A-B). The expression levels of NR4A1 in the livers from WT mice or NR4A1-KO mice treated with LFD or HFD. Melatonin treatment could alleviate the increased NR4A1 level seen with HFD treatment. (C). The oral glucose tolerance test (OGTT) in LFD or HFD mice with or without melatonin treatment. Blood glucose levels were measured immediately before glucose challenge (2 g/kg) and at 30, 60 and 120 min thereafter. (D-I). Plasma triglyceride, total cholesterol, leptin, adiponectin, AST and ALT

levels in different treatment groups. Data are shown as the mean ± SEM. n=6 mice per group. *P<0.05 vs LFD groups; #P<0.05 vs HFD-treated WT mice.

FIGURE 2

Melatonin prevents NAFLD via inhibition of NR4A1. NR4A1$^{-/-}$ mice and WT controls were fed a high-fat diet (HFD) in the presence or absence of melatonin. (A). Liver sections with hematoxylin and eosin (H&E) staining. Hepatic fibrosis according to Sirius Red staining. The hepatosteatosis according to Oil Red staining. The ultrastructure of liver tissues via electron microscopy. (B). The quantification of hepatocyte vaculation. (C). The relative intensity of Sirius Red. (D). The quantification of Oil Red staining. (E). The immunofluorescence of VCAM1 and MMP9. (F-H). The changes in inflammatory factors IL-6, TNFα and TGFβ. Data are shown as means ± SEM. n=6 mice per group. *P<0.05 vs LFD groups; #P<0.05 vs HFD-treated WT mice.

FIGURE 3

Melatonin blocked mitochondrial fission via reducing NR4A1. The palmitic acid (PA, 75 μM for 24 h) was used to mimic high-fat injury in hepatocyte (an equal volume of DMSO was used as the control treatment). Meanwhile, siRNA was used to knockdown the expression of NR4A1 in order to characterize NR4A1 loss-of-function in vitro. The NR4A1 agonist cytosporone B (CsnB, 10 μg/mL) was administered to determine the effects of NR4A1 gain-of function in the face of melatonin treatment. (A). Primary hepatocytes were labeled with Tom20 to determine the mitochondrial fragmentation. (B). To assess changes in mitochondrial morphology quantitatively, the length of mitochondria was measured. (C-E). The change of Drp1 cellular distribution. (F). The co-staining of Drp1 and mitochondria. The mitochondria marked by Drp1 had greater amounts of free debris. However, in NR4A1-silenced cells or melatonin-treated cells, Drp1 foci on the mitochondria were clearly decreased, and the mitochondria maintained almost normal morphology with fewer fragments. Data are shown as the means ± SEM. *$P<0.05$ vs normal group; $^{\#}P<0.05$ vs PA group, $^{@}P<0.05$ vs PA+siRNA-NR4A1 or PA+melatonin groups.

FIGURE 4

Mitochondrial fission induced cellular oxidative stress and calcium overload. (A-B). The mROS was measured to reflect the mitochondrial oxidative stress. (C). The mPTP opening rate was detected by TMRE fluorescence. (D-E). The changes in 10-N-nonyl acridine orange (NAO) fluorescence indicated the cardiolipin (CL) oxidation. In normal cells, NAO could interact with non-oxidized cardiolipin and produces a characteristic green fluorescence. However, after cardiolipin is oxidized, NAO cannot bind to it. (F-H). The changes in MDA, GSH, and SOD levels. (I-J). The cytoplasmic $[Ca^{2+}]$ map via confocal microscopy by Fluo-2. Fluorescence intensity of Fluo-2 was measured by excitation wavelengths of 340 nm and emission wavelengths of 500 nm, respectively. Data (F/F0) were obtained by dividing fluorescence intensity (F) by (F0) at the resting level (t = 0), which was normalized to control groups. Data are shown as means ± SEM. $^{*}P<0.05$ vs normal group; $^{\#}P<0.05$ vs PA group, $^{@}P<0.05$ vs PA+siRNA-NR4A1 or PA+melatonin groups.

FIGURE 5

Melatonin reversed mitophagy activity via upregulating Bnip3. (A-C). The expression and transcription of Bnip3 was regulated by the NR4A1. (D). The co-staining of mitochondria and lysosomes. Loss of Bnip3 could reverse the overlap of mitochondrial debris and lysosomes in melatonin-treated cells. (E-G). Atg5, Beclin1 and mitochondrial LC3II (mito-LC3II) were used to quantify mitophagy activity by western blots. (H). The autophagic flux measurement was conducted via immunofluorescence of mitochondria and LC3II. PA treatment alleviated the merge of mitochondria and LC3II. However, this conformation change was recused by NR4A1 deletion or melatonin treatment. Notably, silence of Bnip3 could cancel the effect of melatonin on mitophagy. $^{*}P<0.05$ vs normal group; $^{\#}P<0.05$ vs PA group, $^{@}P<0.05$ vs PA+siRNA-NR4A1 or PA+melatonin groups.

FIGURE 6

Recovery of mitophagy via melatonin treatment could improve mitochondrial respiratory function. (A). The change in cellular ATP production. (B-C). The mitochondrial membrane potential was

measured by JC-1 staining. (D-H). The OCR assay was used to obverse the mitochondrial respiratory function. Data are shown as the means ± SEM. *P<0.05 vs normal group; $^{\#}$P<0.05 vs PA group, $^{@}$P<0.05 vs PA+siRNA-NR4A1 or PA+melatonin groups.

FIGURE 7

NR4A1 activated p53-mediated mitochondrial fission via upregulation of DNA-PKcs. (A-D). p53 was regulated by NR4A1 and contributed to Drp1 migration and Bnip3 expression. Melatonin had the ability to repress the p53 activation via suppression of NR4A1. *P<0.05 vs normal group; $^{\#}$P<0.05 vs PA group, $^{@}$P<0.05 vs PA+siRNA-NR4A1 or PA+melatonin groups. (E-H). DNA-PKcs was activated by NR4A1. Loss of DNA-PKcs could reduce the p53 activation and reverse mitophagy markers. *P<0.05 vs normal group; $^{\#}$P<0.05 vs PA group, $^{@}$P<0.05 vs PA+siRNA-NR4A1 or PA+melatonin groups. (I) DNA-PKcs deletion maintained the length of mitochondria. (J-L). DNA-PKcs knockout could also prevent the development of NAFLD. H&E staining was used to observe the changes in liver structure. The TUNEL assay indicated that loss of DNA-PK could alleviate the liver injury, as shown by less TUNEL-positive cells. These results were similar to melatonin-treated mice. *P<0.05 vs LFD groups; $^{\#}$P<0.05 vs HFD-treated WT mice.

FIGURE 8

High-fat injury induces NR4A1 upregulation and subsequently activates DNA-PKcs. The latter maintains p53 expression via phosphorylation at the Ser15 site. The activated p53 assists the Drp1 translocation to the mitochondria, forcing mitochondrial fission. Meanwhile, p53 also represses the transcription and expression of Bnip3, impairing the mitophagy activity. The excessive fission and badly structured mitophagy were associated with mitochondrial dysfunction, including energy shortage, mPTP opening, membrane potential collapse, cellular oxidative stress and calcium overload. Melatonin supplementation negates the increased NR4A1 expression and therefore blocks the DNA-PKcs and p53 activation. Through inhibiting the NR4A1/DNA-PKcs/p53 pathways, melatonin reduces the mitochondrial division but increases the mitophagy, maintaining mitochondrial homeostasis in the development of NAFLD.

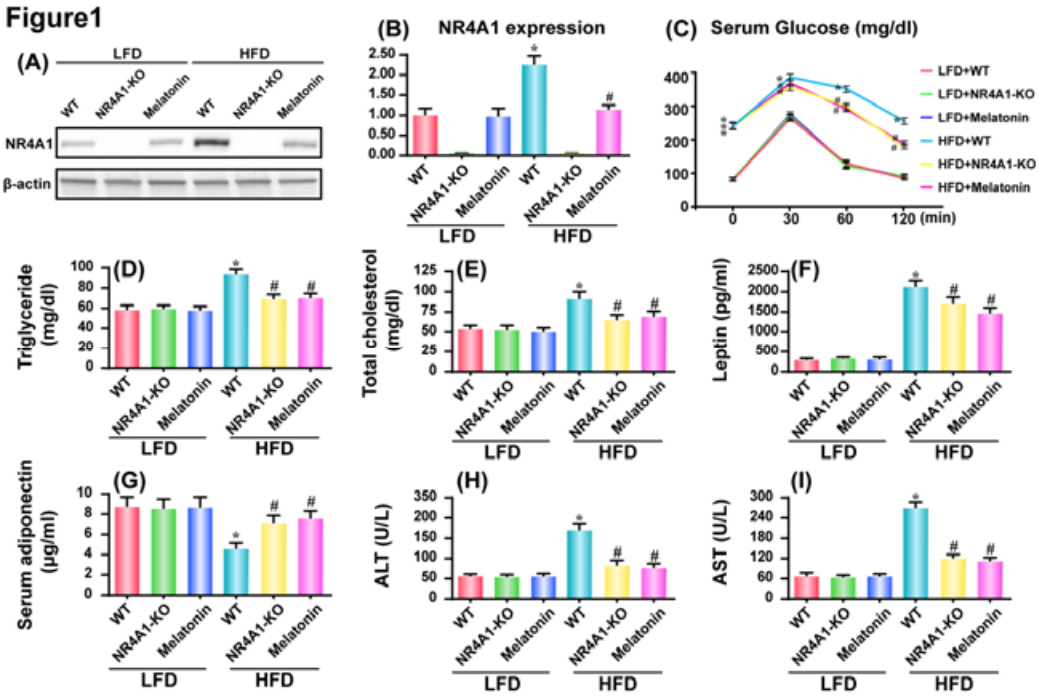

Figure2

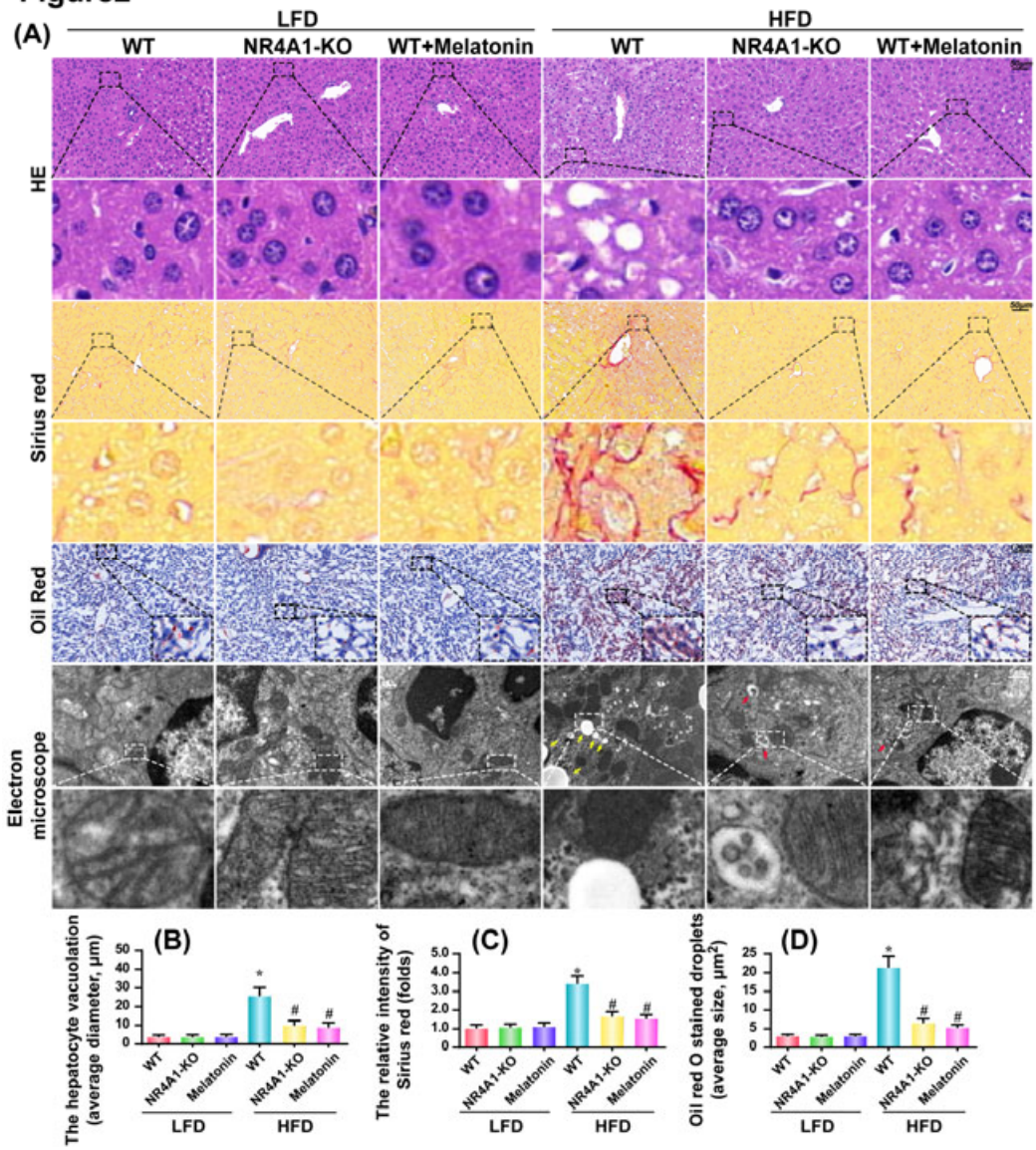

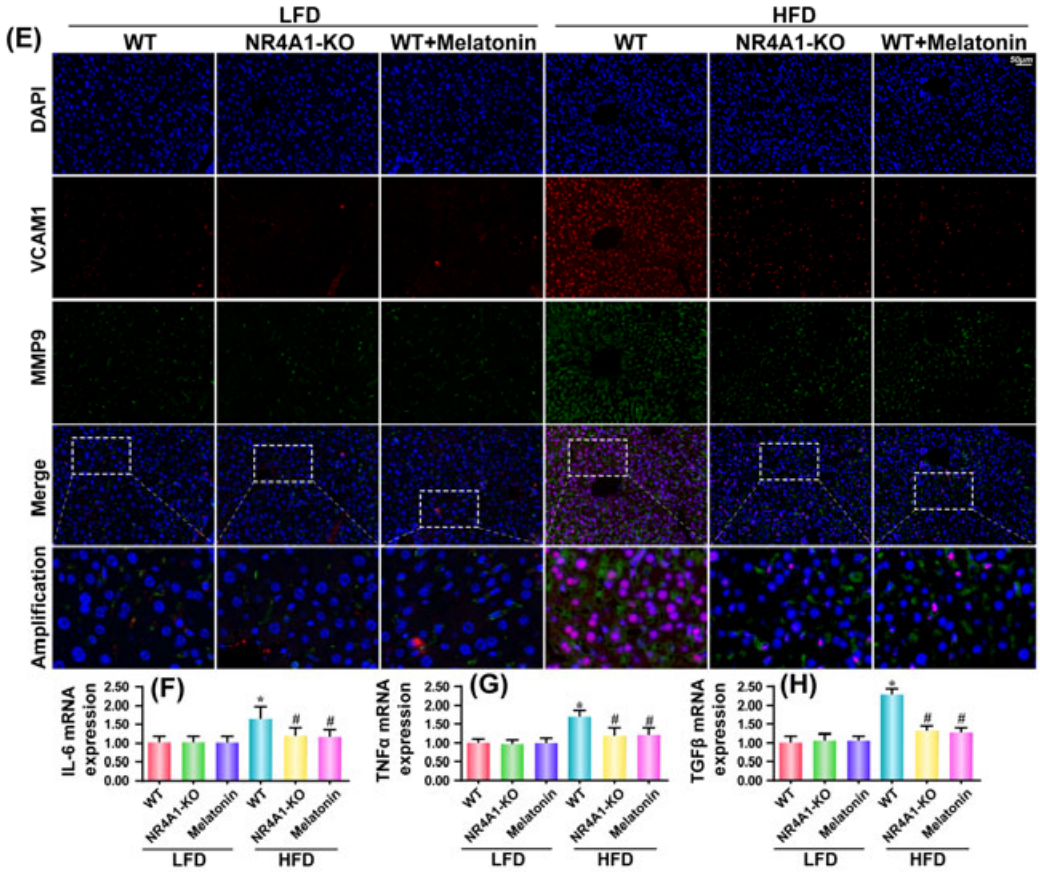

Figure3